Recovery of rare earth elements from NdFeB magnet by mono- and bifunctional mesoporous silica: Waste recycling strategies and perspectives

Oksana Dudarko [a], Natalia Kobylinska [b,*], Vadim Kessler [c], Gulaim Seisenbaeva [c]

[a] O.O. Chuiko Institute of Surface Chemistry NAS of Ukraine, 17, General Naumov Str., Kyiv 03164, Ukraine
[b] A.V. Dumansky Institute of Colloid and Water Chemistry NAS of Ukraine, 42, blvd. Akad. Vernadskogo, Kyiv 03142, Ukraine
[c] Swedish University of Agricultural Sciences, Almas allé 5, Box 7015, 75007, Uppsala, Sweden

ARTICLE INFO

ABSTRACT

Rare earth elements (REEs) such as Nd^{3+} and Dy^{3+} were recovered from simulated and real leaching solution of the NdFeB magnet via solid phase extraction (SPE). Extraction of REEs from simulated solutions was investigated using silica functionalized with NH_2-, EDTA and/or phosphonic groups. The effects of several experimental factors (pH, efficiency of adsorbents, selectivity, and elution of metal ions) on extraction of REEs were investigated. Exploiting specific affinities of adsorbents toward REEs in the presence of competing ions, selective separation of REEs was achieved successfully. The affinity of phosphorous/nitrogen containing adsorbents had the descending order of adsorption: $Fe^{3+} > Dy^{3+} > Nd^{3+} > Ni^{2+} > Al^{3+}$ for multi-component systems. In the first approach, a procedure based on precipitation of Fe^{3+} ions combined with SPE was evaluated for the recovery of REEs in two steps. Most of the Fe^{3+} ions (85%) were efficiently separated by adding an ammonia solution (pH ~ 2.5). Chemical analysis of precipitate showed, though, a high content of REEs. Extraction of REEs from supernatant liquid via bi-functional mesoporous silica with EDTA and/or phosphonic groups recovered ~97.0% of Nd^{3+} with Ni^{2+} and Al^{3+} ions as impurities. Non-ordered silica functionalized with phosphonic groups, showed economical superiority over other mesoporous adsorbents studied for REEs extraction. Complete recovery (97.8%) of REEs was achieved after several stages of SPE with adsorbents functionalized by P/N-containing groups. The in-advance removal of Fe^{3+} ions was a prerequisite for successful implementation of this approach. Finally, separation of Nd^{3+} and Dy^{3+} was performed from nitric acid media using the gradient elution to obtain 98.4% purity Nd^{3+}. The proposed step-by-step SPE procedure by P/N-containing functionalized silica was successfully applied for extraction of REEs (95.5%) in an industrial magnet. This study opens up possibilities for application of the developed approach for the End-of-Life materials recycling.

1. Introduction

Rare-earth elements (REEs) are used in manufacturing wind generators, catalysts for breakdown of harmful exhaust gases, petroleum refining catalysts, hard drives in laptops, headphones, electric vehicles, mobile phones, hybrid engines, laser and magnetic resonance imaging (Alonso et al., 2012). Main challenge in their production lies in difficulties in extraction of the raw materials being an energy-consuming process that can harm the environment leading to its chemical contamination. In addition, a single country, China, has a near-monopoly position in global production of REEs (90% of imports). Prices of Rare Earth oxides and metals rose rapidly in 2010 and 2011, due to restrictions introduced on Chinese exports. For example, the price of

Dy^0 soared from \$250/kg to \$2840/kg, while the price for Nd^0 rose from \$42/kg to \$334/kg (Humphries, 2013). The demand for REEs increases with 9–15% per year and is expected to purge following the rapid development of the market of electric vehicles (Zakotnik et al., 2007).

Several perspective compositions of permanent magnet have been reported (Table 1): samarium cobalt, alnico, ceramic (or ferrite) and NdFeB magnets. The NdFeB-type magnets have replaced alnico and ferrite magnets in many of the modern applications where strong permanent magnets are used (Herbst and Croat, 1991). The NdFeB magnets are high strength combine with relatively low cost.

The End-of-Life (EOL) of NdFeB permanent magnets depends on the application: from 2 to 3 years in consumer electronics to 20–30 years in generators of wind turbines (up to 2000 kg). Therefore, the dumping of

valuable raw materials when the electronic devices have reached their time-of-life limit is wasteful. Recycling of such EOL products with extraction of REEs is very important for the supply of REEs resources in the future (Binnemans et al., 2013; Tunsu et al., 2015; Yang et al., 2017; Judge and Azimi, 2020; Jyothi et al., 2020; Yoon et al., 2016). Furthermore, it needs to be pointed out that determination of REEs in complex solutions containing macro amounts of other metal ions is quite difficult and not trivial with only analytical techniques (Zawisza et al., 2011). Recovery processes must respond to several criteria in order to make recycling the NdFeB magnet-based waste sustainable. These processes must be:

(1) highly efficient on recovering the REEs with high selectivity against Fe and other elements;

(2) applicable to different complicated compositions with various concentrations of REEs;

(3) eco-friendly (e.g. low usage of chemicals and energy with minimum waste generation to the environment).

Different strategies are adopted for EOL magnets (Table 2). The pyrometallurgical processes use high temperatures to convert feed materials into the valuable REE oxides (Firdaus et al., 2016; Okabe et al., 2003). Pyrometallurgy has the drawback of high energy consumption and process temperature, and generation of large amount of *greenhouse gas* emissions. Usually, during hydrometallurgical processes, the waste materials are dissolved with strong acid into an aqueous solution, and then separated and refined to remove impurities. This process may include selective precipitation (Önal et al., 2015; Rabatho et al., 2013), ion exchange and adsorption/solid phase extraction (SPE) (Zhang et al., 2019; Yamada et al., 2018), supercritical fluid extraction (Zhang et al., 2018), solvent extraction (Yoon et al., 2016; Banda et al., 2012; Zhu et al., 2004) in combination with membrane (Kim et al., 2015), electroanalytical techniques (Makarova et al., 2020; Venkatesan et al., 2018), bacteria (Auerbach et al., 2019) for separating individual REEs or their mixtures from the raw concentrate. The solvent extraction is most predominant in separation and recovery of REEs (Yoon et al., 2016; Pradhan et al., 2020). Acidic extractants are commonly used for REEs extraction from aqueous solutions. Two classes of acidic extractants widely used in industry include organophosphorous acids (Gergoric et al., 2017a; Wang et al., 2019) and carboxylic (fatty) acids (du Preez and Preston, 1992; Hoogerstraete et al., 2014). The large amounts of Al and B ($\geq$10%) were co-extracted with TODGA (N,N,N′,N′-tetraoctyldiglycolamide) as an extractant (Gergoric et al., 2017b). In nitrate solutions, TODGA, Cyanex 923, and tributyl phosphate (TBP) have been used to extract REEs with minimal co-extraction of iron (Kim et al., 2015). These extractants have limited selectivity for REEs. Ionic liquids offer a high potential in solvent extraction of REEs (Wellens et al., 2012; Riano and Binnemans, 2015). Although the solvent extraction is the most common unit operation in hydrometallurgical processes, the selective separation of REEs isn't implemented (Hoogerstraete et al., 2014). A previous study (van Loy et al., 2020) examined an alternative approach to the extraction of REEs and Co from NdFeB magnet by mechanical conversion with $Fe_2(SO_4)_3$ using water as solvent, providing REE-oxides in the residue (> 95%). Alternatively, Zhang (Zhang et al., 2018) and Yao (Yao et al., 2017) proposed the supercritical fluid extraction of REEs from EOL products without the need for specific acid leaching or roasting treatment. The main disadvantages of using organic

extractants and solvents are: (i) they produce secondary wastes polluting the environment, (ii) they are quite complex and high time and energy consuming processes. Moreover, Fe^{3+} and other multivalent ions such as Al^{3+} (Wang et al., 2019) in the acidic medium may be co-extracted at high concentrations and high organic to aqueous phase ratios.

Optimization of the solvent extraction process is more complex than SPE for large-scale industrial applications (Jyothi et al., 2020) because the interfacial areas per unit processing volume for mass transfer are lower than those in SPE. Also, the selectivity of adsorbents is determined by the properties of the functional groups on the surface, and by the strength of metal-ligand bond (Queffélec et al., 2012). Typically, most of the adsorbents developed for SPE of REEs are functionalized with P-containing groups and/or ligands used in solvent extraction grafted to solid support (Hu et al., 2018). For example, Ogata et al. (2015–2016) was focused on silica gel framework with a diglycolamic acid as ligands (an analog of TODGA) for adsorption of REEs (Ogata et al., 2015; Ogata et al., 2016). When Fe^{3+} and Al^{3+} ions are present in the same solution, they are also frequently complexed; thus, their co-extraction with REEs virtually always occurs on acidic adsorbents (Ogata et al., 2015). As a result of the metal ion adsorption, the adsorbents modified with succinamic and glutaramic acids adsorbed negligible amounts of REEs, and Fe^{3+} ions were extracted at pH $\sim$ 2.0–2.2 (Ogata et al., 2016). Functional mesoporous supports using phosphonic acid and phosphoric ester derivatives, which demonstrated good extraction behaviour for REEs extraction was described (Queffélec et al., 2012). In comparison, the uses of ion exchange and adsorption processes for REEs recovery are reported significantly less than solvent extraction in hydrometallurgical. Most research has focused on the use of materials that function as cationic exchangers and adsorbents toward REEs in aqueous solutions (Anastopoulos et al., 2016), leachates from ore and fluorescent lamp (Judge and Azimi, 2020). However, limited progress has been made on SPE of REEs from multicomponent system particularly EOL magnet products in applications of practical scale.

In our previous study, bi-functional SBA-15-based materials with phosphonic acid derivatives exhibited excellent adsorption capacity, promising selectivity toward REEs and good chemical stability (Dudarko et al., 2021). It appeared promising for the extraction and concentration of REEs in the presence of transition metals to use sorbents which also contained derivatives of ethylenediaminetriacetic acid (Roosen and Binnemans, 2014). The enhancement of the complexing properties of the compounds by including additional groups in the chelating functional layer allows extending the pH range for extraction. However, this will increase the costs of the process, which is why an economic analysis vs. adsorption characteristics is required to justify this possibility.

In the present study, a different hydrometallurgical approach than described so far was developed to separation and recovery of REEs (Nd^{3+}, Dy^{3+}) from a simulated NdFeB magnet solution. The model multi-component solution was investigated to understand the separation trend (e.g. pH, selectivity) and evaluate the adsorbents' affinity toward transition metals and REEs. Extraction mechanism of REEs and co-extracted ions by adsorbents in a series of silica-based adsorbents was tested and discussed. First, impurities (mainly Fe) were removed by precipitation as hydroxides, while REEs remained in the solution. Then, SPE of the REEs by silica-based adsorbents functionalized with phosphonate and aminopolycarboxylate ligands from the supernatant was

Table 1
Composition and magnetic properties of commercial permanent magnets (SIST EN 60404–8-1, 2015).

Magnet	Composition, % (*w/w*)	BH$_{max}$, MG Oe	B$_r$, kG	H$_{CI}$, Oe	T$_C$, °C
NdFeB	REEs: Nd (28–35%); Pr, Tb, Dy, and Gd: (0–10%); B (1–2%); Ni (0–15%); Al, V, Nb (0–1); Fe ($\leq$68%).	30–52	0.6–1.4	750–2000	310–400
SmCo$_5$	REEs (30–33%): Sm (mainly), Ce, Pr; Co (65–67%).	12–20	0.8–1.1	600–2000	720
Sm$_2$Co$_{17}$	REEs (24–26%): Sm (mainly), Ce, Pr; Co (48–52%); Fe (13–18%); Cu (4.5–12%); Ti, Zr, Hf (0–3.0).	10–32	0.9–1.15	450–1300	750
Alnico	Al (13.-22.3%), Ni (12.5–28.4%), Co (0–42.5%), Cu (2.4—6.3%), Ti (0–8.7%), Nb (0–3%).	1.35–10.5	7.0–11.2	500–2170	860
Ceramic (ferrite)	MO·nFe$_2$O$_3$, n = 4.5–6.5, M = Ba, Sr and/or Pb; La (0–4%), Co (0–2%).	0.8–5.1	0.2–0.4	100–300	460

Notes. BH$_{max}$ - maximum energy product; B$_r$ - remanent magnetic flux density; H$_{CI}$ - intrinsic coercivity; Tc – curie temperature.

Table 2

Summary of approaches for REEs recovery from various magnet products.

Resources of REEs	Leaching (or other approach)	Separation	Results	Refs
Magnet scrap	Liquid metal extraction with Mg—Nd alloy 1073–1273 K in tantalum crucible	Mg^0 as the extraction agent	Nd (97.7% purity)	(Okabe et al., 2003)
NdFeB magnet	H_2SO_4 (14.5 M) leaching at 25 °C, drying (24 h at 110 °C), selective roasting (1 h or 2 h) at 750 °C	water leaching (0.02 mg/l at 25 °C)	REEs (98% purity)	(Önal et al., 2015)
Magnetic waste sludge	1 M HNO_3 + 0.3 M H_2O_2	Fe removed as $Fe(OH)_3$ at pH 3 / precipitation of Nd/Dy with $H_2C_2O_4$	REEs (68%): 69.7% (Nd), and 51% (Dy).	(Rabatho et al., 2013)
Postconsumer NdFeB magnets (wind turbines	supercritical CO_2 as the solvent	the TBP–HNO_3 chelating agent and 2 wt% CH_3OH	Nd (94%), Pr (91%), Dy (98%) with co-extraction of Fe (62%)	(Zhang et al., 2018)
Waste neodymium magnet	0.1 mol L^{-1} H_2SO_4 at 50 °C, 24 h and stood for 1 h at 0.1 g/100 mL	Fe^{3+} separated by $H_2C_2O_4$, separation Dy and Nd/Pr by chromatographic separation and elution	Nd (91% purity)	(Yamada et al., 2018)
NdFeB and industrial scrap magnets	1–6 M HNO_3 and 3–6 M HCl	Membrane assistant solvents extraction (TODGA, Cyanex 923, TBP) and Isopar L (solvent)	REE(Nd, Pr)$_2O_3$ by precipitation with $H_2C_2O_4$	(Kim et al., 2015)
NdFeB magnet waste	HCl (37%): nHCl/nREEs = 3.5	Membrane electrolysis: Fe^{2+} was oxidized in the anode, precipitated ($Fe(OH)_3$) (undissolved magnet further until ≥95%), REEs precipitated by $H_2C_2O_4$ (1: 2)	REE_2O_3 with a purity ≥99.5% (Co, Al as impurities).	(Venkatesan et al., 2018)
EOL magnets (MQU-F sintering powder, slices, e-motors)	Bioleaching with *Acidithiobacillus* and *Leptospirillum ferrooxidans* (14 days): slices leached with efficiency 44% (Dy) and 90% (Nd) / non-selective leaching by the bacteria	Separation with precipitation by $H_2C_2O_4$ (conc.) and extraction with *Cyphos IL101* subsequently D2EHPA (to remove the Al, B and Cu) treatment	REEs (near 100%), purity 98%.	(Auerbach et al., 2019)
NdFeB waste	H_2SO_4 (Nd, Dy, Pr, Gd, Co, and B)	Solvent extraction by 0.3 M or 1.2 M D2EHPA in either octane or hexane/stripping of REEs from organic phases using HCl (2 M or higher)	Dy and Gd (~50%)	(Gergoric et al., 2017a)
Neodymium magnet powder	HNO_3	Extraction of REEs (Nd, Dy and Pr) with TODGA (0.1 M) in Solvent 70 (C11–C14 ≤ 0.5% (w/w), hexane, toluene and 1-octanol (Al, B ≥ 10%)/ Extraction of REEs using MQ	REEs (98%).	(Gergoric et al., 2017b)
Used NdFeB permanent magnets	HNO_3 (5 mL, 65%) and water (10 mL)	Extraction of REEs (Nd, Dy) using EDTA with IL (*Cyphos IL101*), precipitated REEs and Co by $H_2C_2O_4$, calcination	Nd_2O_3 (99.6%), Dy_2O_3 (99.8%) and CoO (99.8%)	(Riano and Binnemans, 2015)
Cylindrical NdFeB magnets	mechanochemical grinding of the NdFeB (powder) and $Fe_2(SO_4)_3$/ leaching powder (REEs, Fe and Co) in H_2O	REEs precipitating by $H_2C_2O_4$; calcination	leaching yield of REEs (>95%), full recovery of Co	(van Loy et al., 2020)
NdFeB magnet wastes	(a) 7.0 g + 100 mL, 1.0 M HNO_3 for 36 h (pH 4.7) at 343 K; (b) 40.0 g + 100 mL, 6.5 M HNO_3 for 48 h (pH 2) at 343 K	precipitation of $Fe(OH)_3$ by NaOH(1.0 M, pH 4.5) / extraction of REEs (Pr, Nd and Dy) by 1.8 M TBP with IL (tricaprylmethylammonium nitrate)	C(Nd) = 10 g L^{-1} after 7 repeated contacts in the 5.0 M $NaNO_3$	(Kikuchi et al., 2014)
NdFeB magnet wastes without iron oxide (oxidative roasting)	High heat-treated with BN		C(Nd) = 60 g L^{-1} after the third repeat in the 2.0 M $NaNO_3$	

Abbreviations. TBP - Tri-*n*-butyl phosphate; *TODGA* - N,N,N′,N′-tetraoctyldiglycolamide; *IL* - ionic liquid; *Cyphos IL101* - trihexyl(tetradecyl)phosphonium nitrate; *D2EHPA* - di-(2-ethylhexyl) phosphoric acid; *Cyanex 923* - commercial mixture of trialkyl phosphine oxides, with C6 and C8 chains; E*DTA* - ethylenediaminetetraacetic acid, MQ – MQ water.

performed. Subsequently, elution of REEs from the solid phase to aqueous phase designed for controlled release of Nd^{3+} and Dy^{3+} was used. Second, the proposed series of silica-based adsorbents were evaluated for step-by-step SPE of impurities and target REEs from the simulated solution. The optimal conditions for the removal of metal ions using various adsorbents were tested. Recovery of REEs was then investigated using elution of adsorbents. Basic criteria tested for such a recovery to be effective is achieving over 90% REEs extraction with co-extraction of less than 5% Fe. The separation of Nd^{3+} from Dy^{3+} in the effluent solution was also investigated. Finally, the optimized hydrometallurgical approach was applied for the recovery REEs from the real magnet.

2. Experimental

2.1. Materials and reagents

Iron standard solution, 1000 mg/L Fe in 0.5 M nitric acid (from Fe $(NO_3)_3$) Certipur® standard for AAS, Supelco® was obtained from Merck. Acids, bases, EDTA, thiocyante, REE and base metal slats were supplied by Merck, Sigma-Aldrich or Supelco: HCl (ACS reagent, 37%, Merck), HNO_3 (65.0–67.0%, Merck), $Nd(NO_3)_3 \cdot 6H_2O$ (99.9%, Sigma-Aldrich); $Fe(NO_3)_3 \cdot 9H_2O$ (≥98%, Sigma-Aldrich); $Dy(NO_3)_3 \cdot 6H_2O$

(99.9%, Sigma-Aldrich); $Ni(NO_3)_2 \cdot 6H_2O$ (99.9%, Sigma-Aldrich); H_3BO_3 (99.5%, Sigma-Aldrich); $Al(NO_3)_3 \cdot 9H_2O$ (97%, Sigma-Aldrich), ethylenediaminetetraacetic acid (EDTA, purified grade, ≥98.5%, Sigma-Aldrich), NaOH (≥98%, pellets (anhydrous), Merck), NH_3/H_2O (25%, Sigma-Aldrich), KSCN (99%, Merck), $Ca(OH)_2$ (≥96%, Sigma-Aldrich), Arsenazo III (Supelco). For all purposes, pure and ultrapure water from Merck Milli-Q® Integral system was used.

2.2. Characterization and chemical analyses

Fourier transform infrared (FTIR) spectra were recorded from the samples pressed into pellets with KBr or pure silica using a *Nicolet Nexus 470* (Thermo, USA) spectrometer. A Specac Variable-Temperature cell P/N 21525 was used for the thermal measurements (for temperatures from 20 to 200 °C). Powder XRD data were obtained using a PAN Analytical X'Pert PRO apparatus equipped with an X'Celerator detector with automatic data acquisition (X'Pert Data Collector (v2.0b) software) using monochromatized CuKα (λ = 1.5406 Å) radiation. The pH of suspensions was measured on 1120-X pH-meter (Mettler-Toledo).

Metal ion concentrations in solution were determined by inductively coupled plasma optical emission spectrometry (ICP-OES, iCAP 6300 (Thermo Scientific, USA)) and spectrophotometry (Shimadzu UV-1800, Japan). An ICP-OES was used for the determination of trace metal ions.

Also, the concentration of Fe^{3+} and Nd^{3+} ions was determined by spectrophotometry in reaction with KSCN (470 nm) and Arsenazo III (672 nm), respectively. Screening analyses of metal ions in solid and liquid phase were performed by semi quantitative EDX techniques (Hitachi TM-1000-μ-DEX, Japan).

2.3. Precipitation, adsorption and desorption

Precipitation of Fe^{3+} ions from simulated solutions was performed using $Ca(OH)_2$ or $NH_3(aq)$. In this case, the pH of the simulated solution was adjusted to 1.60 by sodium hydroxide, and then mixture was reacted with precipitate (1 mL base/10 mL simulated solution) slowly added until pH near 3 (in 15 min) at room temperature. The obtained precipitates and supernatant were separated by filtration.

Batch sorption experiments were carried out in a series of 25 mL glass flasks containing 10–15 mL solution of an individual or mixture of metal ions. Predetermined amounts of adsorbents (0.1–0.25 g) were added to the test vessel. All the experiments were performed in a thermostatically controlled shaker, maintained at 200 rpm and a pre-set temperature of 25 °C. Based on the results from preliminary kinetic studies, a stirring time in the range 1 h to overnight was selected as the equilibration time for all sorbents. On completion of the sorption experiments with functionalized silica, the samples were filtered through filters to separate the silica particles from the aqueous phase. The metal ion concentration in the filtrate and washed liquor was analysed using ICP-OES while the adsorbent washed with deionized water was investigated by EDX analysis.

The adsorption capacity (q_e) and recovery were calculated using the following equations:

$$q_e \left(mg\ g^{-1}\right) = \frac{(C_0 - C_e) \bullet V}{m} \bullet A_r$$

$$Recovery\ (\%) = (C_0 - C_e) / C_0 \bullet 100\%$$

where, C_0 and C_e are the initial and equilibrium concentrations of the metal ions (mol dm^{-3}), respectively; A_r is the molar mass of the element (g mol^{-1}); V is the volume of the solution (dm^3); and m is the weight of the solid (g).

The selectivity coefficient ($S_{Nd^{3+}/M}$) was calculated from equation:

$$S_{Nd^{3+}/M} = K_{d_{Nd^{3+}}} / K_{dM}$$

where, $K_{dNd^{3+}}$ and K_{dM} were the distribution coefficients of the Nd^{3+} ions and other metal ions in mixture, respectively.

In a typical experiment, adsorbent was contacted with 1–5 mL of HNO_3 solution (0.1–1.0 M) as eluting agent and contact time with stirring (0.5–24 h) at room temperature. Then the suspension was centrifuged during 5 min. After centrifugation at 10,000 rpm, the quantitative desorption of metal ions in the supernatant was determined by ICP-OES. Reconditioned samples were used in sequential extraction experiments, repeating the adsorption and desorption procedure.

2.4. General methodology

Our experimental procedure had two main directions. In the first direction, the precipitation method was utilized in order to eliminate major amount of macro impurities (especially Fe and Al), that hinder the adsorption of REEs from simulated NdFeB magnet solution (Fe, Nd, Dy etc.). In the second direction, various adsorbents were evaluated for step-by-step separation of interfering macro impurities (first stage) and then of target REEs ions (second stage). The summary REEs recovery route from magnet wastewater proposed in this work is presented in Fig. 1.

The flowsheets start with preparation of simulated magnet solution as model. The top two parts (left and right) of first stage of the flowsheet
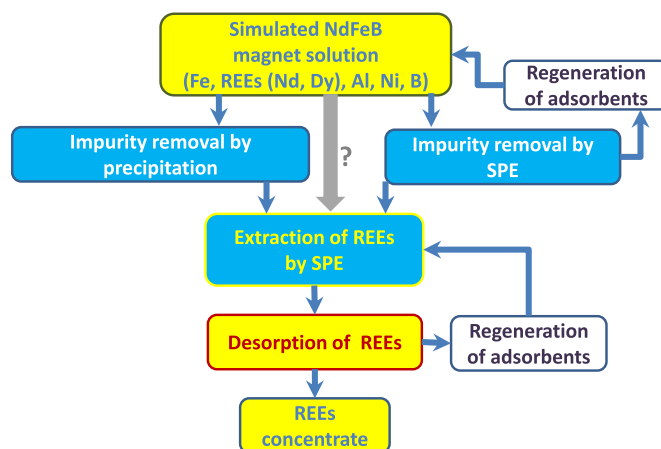

Fig. 1. Schematic presentation REEs recovery from simulated NdFeB magnet solution by proposed hydrometallurgical processes.

in Fig. 1 have conceptual differences. In the left side of the flowsheet, the magnet solution was treated with alkaline solution ($Ca(OH)_2$ or $NH_{3(aq)}$) in the beginning at room temperature and then heated at 100 °C (5 min). The formed Fe/Al-contained precipitate was separated from the REEs-dominated supernatant solution by filtration. In the right side of the flowsheet, macrocomponents such as Fe were selectively extracted from the simulated magnet solution by several adsorbents. The Fe-loaded adsorbents were regenerated and reused several times. In the middle stage, a similar approach was used for REEs-containing liquor with several impurities. In this stage REE metal ions were separated by selective SPE using functionalized mesoporous adsorbents. Best conditions for extracting REEs and corresponding desorption were achieved after several optimizations in this study. Overall operation already resulted in a pure REE-containing concentrated solution after desorption stage. The regeneration of adsorbents was studied for life cycle prolongation of materials.

3. Results and discussion

3.1. Composition of the simulated magnet solution

The simulated NdFeB magnet solution was prepared based on the composition achieved from manufacturing company (Sweden) and compared to literature (Tunsu et al., 2015), and composition is shown in Table 3. The initial pH of simulated solution was ~0.68.

The pH of solutions is a critical parameter in the extraction of metal ions because it can affect the properties of both adsorbents (e.g. acid-base properties of the silica matrix, functional group charge, zwitterion state, etc. (Han et al., 2007)) and metal ions (Nordstrom, 2000). This, in turn, can influence the adsorbents' affinity to the target ions and its charge in solution.

Distribution of metal ions and other possible hydroxo-complex species in aqueous solution has been determined as a function of pH and calculated with MINTEQ 3.1 (Fig. 2).

Fig. 2 shows that Fe^{3+}, Al^{3+} ions are only dominant at very acidic conditions (pH < 1.0), while the metal-hydroxo ions are dominant in the

Table 3
Chemical composition of the simulated NdFeB magnet solution.

Concentration	Element						
	Fe^{3+}	Al^{3+}	Nd^{3+}	Ni^{2+}	Dy^{3+}	B^{3+}	Total
C, mmol L^{-1}	59.4	0.27	27.7	4.01	2.76	5.71	–
ϖ, %	56.10	0.23	35.69	2.86	3.75	1.38	100.00

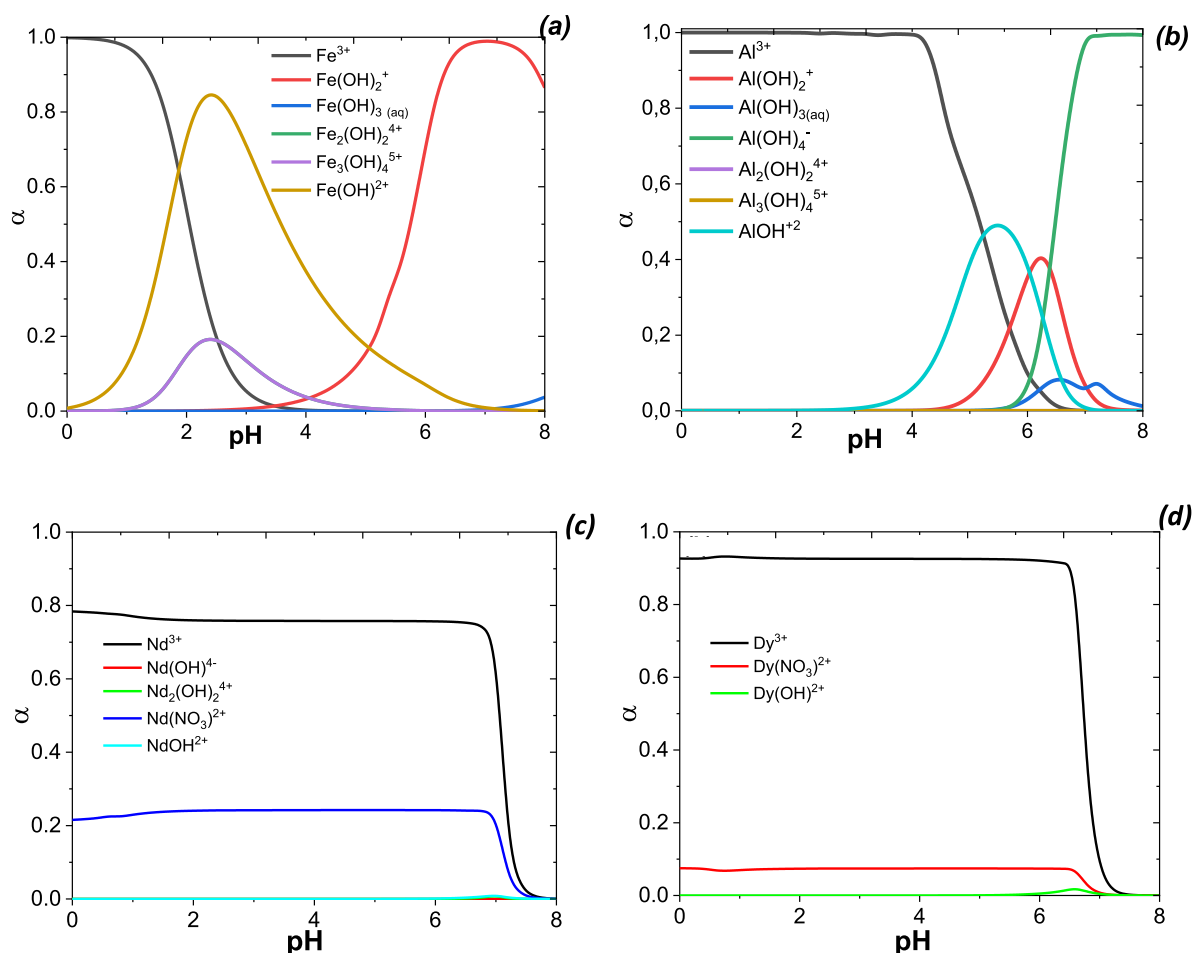*Notes.* In 0.2 M HNO_3; C - molar concentration, mmol L^{-1}; ϖ - mass fraction, % (w/w).

Fig. 2. Speciation of Fe^{3+}(*a*), Al^{3+}(*b*), Nd^{3+}(*c*) and Dy^{3+}(*d*) forms as a function of pH. Conditions: $C(Fe(NO_3)_3 = 59.4$ mol L^{-1}, $C(Al(NO_3)_3 = 0.27$ mol L^{-1}, $C(Nd (NO_3)_3 = 27.7$ mol L^{-1} and $C(Dy(NO_3)_3 = 2.76$ mol L^{-1}.

pH ranges 1–4.5 for Fe^{3+} and 3–6 for Al^{3+} ions. When pH increases, iron is hydrolyzed and precipitated at pH > 2 (pK$_h$ = 2.2 (Khoe et al., 1986; Stefaánsson, 2007)), whereas Al^{3+} hydrolyses at pH ~ 4.5–5.0 (pK$_h$ = 9.7 (Khoe et al., 1986)). Thus, both Fe^{3+} and Al^{3+} ions show solubility minima at near-neutral conditions (pH ~ 5–5.2). Until pH 6, Nd^{3+}, Dy^{3+} ions are the predominant species which present in the solution. With further increase in pH, the corresponding REEs ionic species exist as $NdOH^{2+}$ and $DyOH^{2+}$, dominating in their maximum concentration around pH 9–10.

It should be noted also that the pH of precipitation of metal ions in an individual solution and mixture does not coincide. It is therefore necessary to find an optimum pH range for effective removal of the desired metal ions.

3.2. Adsorbents and their characteristics

It is known (Galarneau et al., 2001), that the adsorption characteristics of silica structures are mainly determined by porosity and the surface layer composition. In our previous studies (Dudarko et al., 2021; Dudarko and Zub, 2017), we described the synthesis and characterization of mesoporous SBA-15 type materials with different P/N-containing functional groups (Dudarko et al., 2021). The main physicochemical parameters for the studied samples are summarized in Table 4.

Previous study used functionalized adsorbents obtained by template method with the polyalkylene oxide-type triblock copolymers as the mesopore-directing agents under acidic conditions (Dudarko et al., 2021). One of them was monofunctional mesoporous silica with EDTA

groups (*SBA/EDTA*). Other two bi-functional samples such as mesoporous silica with EDTA groups combined with phosphonic (*SBA/EDTA/PO$_3$H$_2$*) or protonated aminopropyl groups (*SBA/EDTA/NH$_2$*) are described in Table 4. The economic cost of the synthesis of adsorbent with EDTA and other functional groups was also evaluated (**Table S1**). The estimated total price indicated that the use of sol-gel method considerably decreases the cost of synthesis by 50%. Thus, monofunctional silica with phosphonic groups (*SiO$_2$/PO$_3$H$_2$*) synthesized by sol-gel method was selected as a low-cost adsorbent for the REEs recovery.

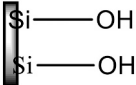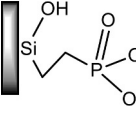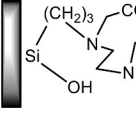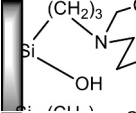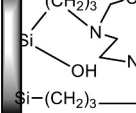The highest value of the maximum adsorption capacity for metal ions was observed for the *SBA/EDTA/PO$_3$H$_2$* sample (Dudarko et al., 2021), reaching 119 mg g^{-1} for Fe^{3+} (pH 2.2), 247 mg g^{-1} for Cu^{2+} (pH 4.5), 238 10 mg g^{-1} for Nd^{3+} (pH 3.5–6.0) and 243 90 mg g^{-1} for Dy^{3+} (pH 3.5–6.0).

In order to use the most suitable conditions for the extraction of target REEs in the simulated magnet solution, the sample volume and weight, selectivity, eluent type, concentration, and volume were characterized for selected sorbents.

The effect of liquid to solid (L/S, mL/g) ratio on the effective extraction of impurities and target REEs by studied adsorbents was investigated using *SiO$_2$/PO$_3$H$_2$* sample as an example and the results are shown in Table 5.

The adsorption of metal ions at *L: S* = 1000 *mL/g* was significantly higher compared to *L: S* = 3000 *mL/g* for *SiO$_2$/PO$_3$H$_2$* sample (Table 5 and **Fig. S1**). Also, the adsorption efficiency of *SiO$_2$/PO$_3$H$_2$* toward REEs increases at neutral pH with the decrease in L/S ratio. Thus, effectiveness of adsorbents toward studied metal ions was higher with *L: S* =

Table 4
Main textural and chemical parameters of adsorbents.

Sorbent	Matrix	Functional layer	d^1, nm	h_w, nm	S_{BET}, m²/g	V_{tot}, cm³ g⁻¹	d^2, nm	C_L, mmol g⁻¹
SBA (Dudarko and Zub, 2017)	SBA-15 (ordered)		n.a.	n.a	616	0.73	5.6	–
SiO_2/PO_3H_2 (Dabrowski et al., 2007)	Xerogel (non-ordered)		9.7	1.4	440	0.29	2,2¹	1.57
SBA/EDTA (Dudarko et al., 2021)			9.2	1.4	733	1.00	6.6	0.33
SBA/EDTA/PO_3H_2 (Dudarko et al., 2021)	SBA-15 (ordered)		n.a.	n.a.	633	0.97	6.6	1.27/0.35 (EDTA)
SBA/EDTA/NH_2 (Dudarko et al., 2021)			11.3	1.7	710	1.03	6.6	0.10/0.32 (EDTA)

Notes: d^1 – pore parameters evaluated from XRD data (Baerlocher et al., 2007), nm; h_w – wall thickness of pores, nm; S_{BET} – specific surface area calculated by BET method (Brunauer et al., 1938), m²/g; V_{tot} and d^2 – total volume and diameter of pores evaluated by BJH method (Barrett et al., 1951), respectively, cm³ g⁻¹ and nm; ¹d_{eff} – diameter of pores calculated by Hurwich's formula ($d_{eff} = 4 V/S_{BET}$), nm; C_L - concentration of functional groups obtained by pH-metric titration, mmol g⁻¹, *n.a.* – not available.

Table 5
Effect of L/S ratio on recovery of metal ions in simulated solution by SiO_2/PO_3H_2 sample.

L/S ratio, mL/g	Metal ion recovery at different pH				
	pH 2.2		pH* 5.0		
	Fe^{3+}	Nd^{3+}	Dy^3	Nd^{3+}	Dy^3
3000	67.56	0.92	0.52	79.92	73.52
1000	99.99	1.14	0.57	94.14	92.57

Notes. *-after separation of precipitate. *Conditions*: C(Fe(NO₃)₃ = 59.4 mol L⁻¹, C(Nd(NO₃)₃ = 27.7 mol L⁻¹ and C(Dy(NO₃)₃ = 2.76 mol L⁻¹.

1000 *mL/g*.

To evaluate affinity of studied adsorbents to the REEs, distribution and selectivity coefficients were calculated (Table 6). The selective separation of the adsorbents according to target REEs was achieved by mixing target Nd^{3+} ions with various amount of interfering ions from binary mixtures (Nd^{3+}/Al^{3+}, Nd^{3+}/Fe^{3+} and Nd^{3+}/Ni^{2+}) in batch adsorption experiments.

The selectivity coefficient of Nd^{3+} over each individual base metal ion was far greater than 10 with the exception of Fe^{3+} ions (Table 6). The results demonstrated that the separation of Nd^{3+} from mixed Nd^{3+}/Fe^{3+}

solution was impossible, especially at low metal ion concentrations such as the 1.0 mmol L⁻¹. The observed effect most likely owing to their different affinities to interact with EDTA groups of adsorbents according to stability constant of complexes of each metal ion (Anderegg, 1977). The stability constants of some of these ions follow the descending order: Fe^{3+} (logK = 25.1) > Dy^{3+} (logK = 17.8) > Al^{3+} (logK = 16.0). Also, this statement is supported by '*Hard and Soft Acids and Bases*' theory. The $S_{Nd/Al}$ value reached 659.8 with the adsorbed amount of Nd^{3+} of 139.8 mg g⁻¹ contrasting to that for Al^{3+} ions (4.5 mg g⁻¹) for *SBA/EDTA/PO_3H_2* (pH 2.0). The values of $S_{Nd/Ni}$ ranged from 33.1 to 517.5, and that clearly indicating that it would be easy to separate Nd^{3+} from the mixture of these ions over the whole range of metal ion concentration. Generally, the selectivity coefficients of *SBA/EDTA/PO_3H_2* sample are higher than that of SiO_2/PO_3H_2.

Desorption of metal ions. Desorption of the metal ions from the surface of the adsorbents was investigated using HNO_3 with various concentrations (**Table S2,** Fig. 3).

As shown in Fig. 3, the quantitative desorption of metal ions from investigated adsorbents using 0.1 M nitric acid was not observed. The amount of the residual Fe^{3+} equals to the content of the functional groups in these samples (Table 4). From this point of view, main interaction of Fe^{3+} ions with functionalized mesoporous silica can be

Table 6
Effect of adsorbents for selectivity Nd^{3+} ions over base metal ions.

pH	Sorbent	C_{Nd}, mmol L⁻¹	C_M, mmol L⁻¹	Nd^{3+}/Al^{3+}		Nd^{3+}/Fe^{3+}		Nd^{3+}/Ni^{2+}	
				q_e(Nd), mg g⁻¹	$S_{Nd/Al}$	q_e(Nd), mg g⁻¹	$S_{Nd/Fe}$	q_e(Nd), mg g⁻¹	$S_{Nd/Ni}$
		1.0	1.0	59.2	161.0	20.8	0.05	59.8	33.1
	SBA/EDTA/PO_3H_2	2.0	5.0	139.8	659.8	133.4	1.98	160.0	517.5
	SiO₂/PO₃H₂	1.0	1.0	49.2	24.9	28.0	0.02	50.0	16.7
2.0		2.0	5.0	99.9	162.2	95.5	0.76	130.0	551.3
	SBA/EDTA/PO_3H_2			159.8	218.1	135.5	-*	155.9	261.5
5.5	SiO₂/PO₃H₂	2.0	5.0	129.9	264.6	133.4	-*	129.1	397.0

Notes. *-not determined by account of precipitation effect (Fig. 1). *Conditions*: S/L ratio 1000 mg/L, temperature 25 °C, stirring rate 2000 rpm.
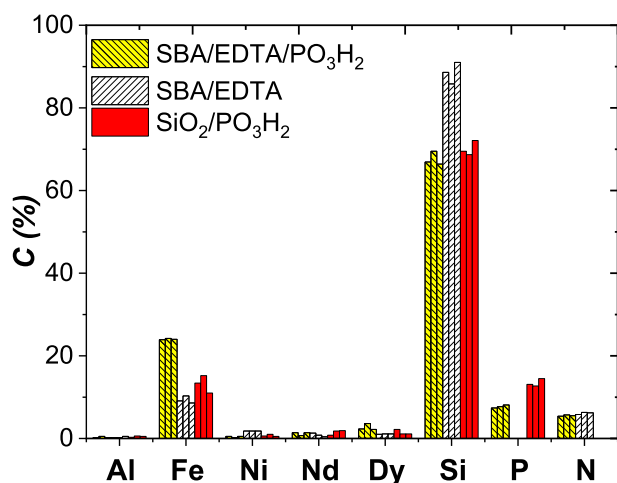
Fig. 3. Summarized EDX elemental analysis of samples after desorption by HNO_3.

explained by complexation and ion-exchange mechanism.

The quantitative desorption from metal-loaded adsorbents was reached by increasing the HNO_3 concentration (*Table S2*). A complete recovery of Fe^{3+} and REEs was achieved with 1.0 M and 0.5 M HNO_3, respectively, during overnight contact. Additionally, eluent volumes between 1.0 and 5.0 mL were employed. Recoveries of the REEs were quantitative at eluent volumes above 1.0 mL. Therefore, 1.0 mL of 0.5 mol L^{-1} HNO_3 was used for elution of REEs in the remainder of this study.

Pre-concentration factor toward REEs was calculated as the ratio of the highest volumes of initial solution (100 mL) to the lowest eluent volumes (1 mL) and was equal to 100.

Alternatively, Fe^{3+} ions can be desorbed from adsorbents, using solutions of strong chelating agents such as EDTA with concentrations varying from 0.5 M to 1.5 M. Quantitative desorption of Fe-loaded adsorbents was ultraslow and attained completeness in around 24 h. It was found that EDTA as eluent demonstrates the increased amount of adsorption/desorption cycles of adsorbents.

3.3. Procedure based on precipitation of impurities combined with SPE of REEs

3.3.1. Precipitation of impurities

In the first stage (Fig. 4), we selected the precipitation as the removal method of undesired Fe^{3+} ions from simulated NdFeB magnet solution, in the form of hydroxide,. Typically, iron(III) hydroxide precipitate is amorphous, low-cost with low value of the solubility product constant ($K_{sp} = 4 \times 10^{-38}$ at 25 °C (*Descriptive Inorganic Chemistry Researches of Metal Compounds*, 2017)). A wise choice of precipitator with optimum pH is capable to provide a iron(III) hydroxide precipitate without co-precipitation of REEs. We observed that the REEs (Nd and Dy) in the simulated solution were precipitated at higher pH (Fig. 2), i.e. all these forms were soluble under these conditions (pH $\leq$ 7.0).

We noted that the pH values of maximum precipitation of Fe^{3+} and Al^{3+} ions do not coincide, i.e. optimum pH removal Fe is pH = 2.5, while for Al ions it is pH = 5 (Fig. 2). Hence, pH of 2.5 was used for the removal of Fe^{3+} ions by precipitation.

As demonstrated earlier (Krupińska, 2019), calcium hydroxide can be used to accelerate the precipitation of Fe^{3+} in the form of $Fe(OH)_3$. This approach to remove Fe^{3+} from simulated magnet solution was evaluated. In this case, we obtained a mixture of red-white precipitates, containing mainly Ca^{2+} and Fe^{3+} ions (*Fig. S2*). The EDX data show that precipitate contain 44–47% Ca, 18–23% Fe, 25–30% Nd, 3–8% Dy, 0.5–3% Ni and 1.1–3.5% Al, all expressed as atom% (or mol%). However, in our case, high concentration of Ca^{2+} ions was observed not only in the precipitate, but also in the centrifuged supernatant solution (91–97%). That's why we decided to change the precipitant from Ca
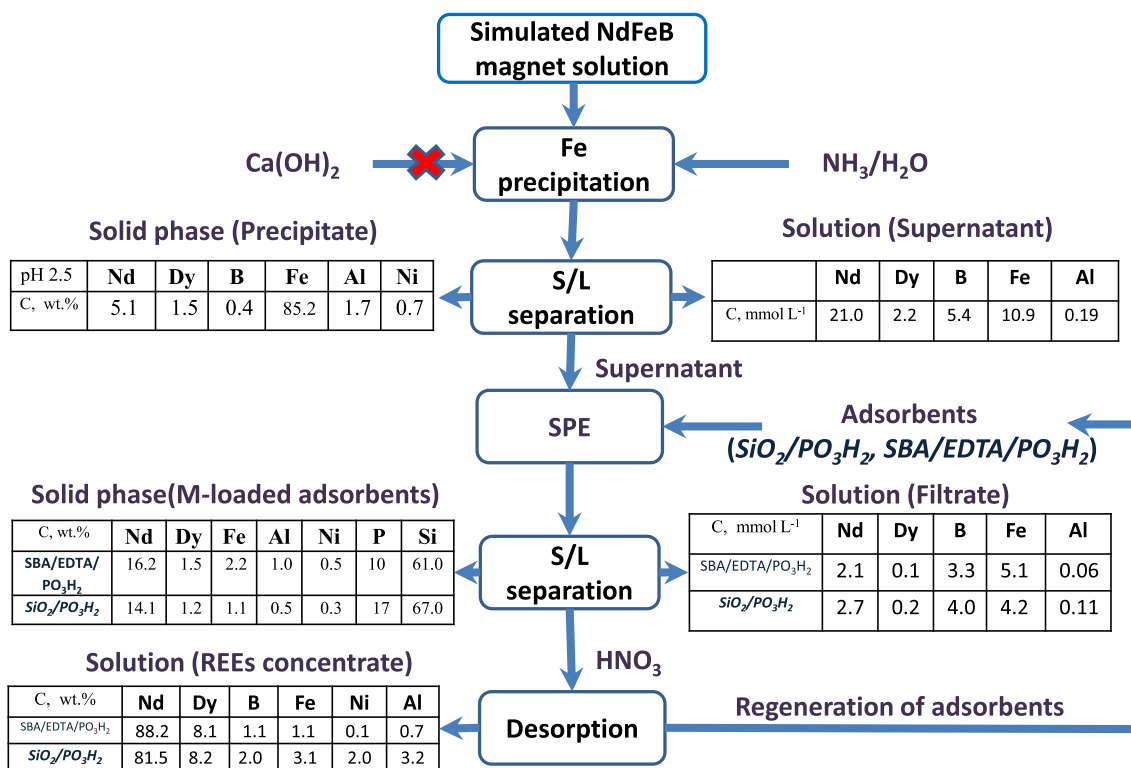

Fig. 4. Schematic representation the process of REEs recovery based on precipitation of Fe^{3+} combined with SPE of REEs from simulated magnet solution.

(OH)$_2$ to NH$_3$(aq) for the removal of main impurities from the simulated solution. The obtained orange precipitate was centrifuged, and washed three times (**Fig. S3**). The orange color of precipitate is characteristic for Fe(OH)$_3$. The XRD spectra indicate that the main phases of the precipitate are amorphous. Likewise, some broad peaks were observed, indicating the presence of the crystalline phase (dominant α-FeOOH or Fe$_3$O$_4$), as shown in Fig. 5.

According to EDX data the obtained precipitates contains up to 75.2% of Fe^{3+}, 2.1% of Al^{3+}, and 10.1% of Nd^{3+} (Fig. 6a). To completely remove impurities (Fe^{3+} and Al^{3+} ions), the obtained solution was treated again by ammonia (**Fig. S4**).

According to the ICP-OES analysis of the metal ion concentrations of supernatant in Table 7, it was possible to precipitate near 82% of Fe^{3+} and 60% of Al^{3+} compared to initial simulated solution. But Nd^{3+} and Dy^{3+} ions were co-precipitated with main impurities or entrapped in iron hydroxide precipitate. The amount of co-precipitated REEs decreased slightly when the solution was refluxed for several minutes. It seems that the presence of Al^{3+} in the samples favours the coagulation process with co-precipitated REEs at this stage. Thus, the presence of Al^{3+} ions is a challenge for this approach.

Thus, the filtrate (or supernatant liquid) after precipitation of metal ions at pH 2.5 contained REEs, in which the main impurities were significantly reduced (Table 7). In the next stage, the supernatant was used for the recovery of REEs.

3.3.2. Recovery of REEs

The SPE experiments using selected adsorbents were conducted using solutions containing Nd^{3+}, Dy^{3+}, Ni^{2+} and Fe^{3+} ions. With increasing pH, the adsorption capacities toward both Nd^{3+} and Dy^{3+} ions were also increased (Dudarko et al., 2021), indicating that acidic conditions are leading to protonation of active sites thus hindering adsorption of REEs. As shown in Fig. 1, the hydroxide species of Nd^{3+} and Dy^{3+} ions, undergo a dramatic increase in solution of pH higher than 6.0. Thus, the best conditions for SPE of REEs were chosen at pH 4.0–5.0. The elemental EDX mapping and analysis of metal-loading on adsorbents after SPE in the supernatant liquid are shown in Fig. 7.

The results show that a high quantity of REEs was extracted from the supernatant liquid, but other metal ions also appeared in negligible concentrations (Fig. 7). The experimental data prove that REEs contained Al^{3+} impurity (on average 0.01–0.12 wt%). Regardless of the EDX mapping, non-regular distribution of REEs on the silica surface was observed. This phenomenon can be explained in terms of the phosphonic groups which are non-homogeneously distributed on the surface of silica.
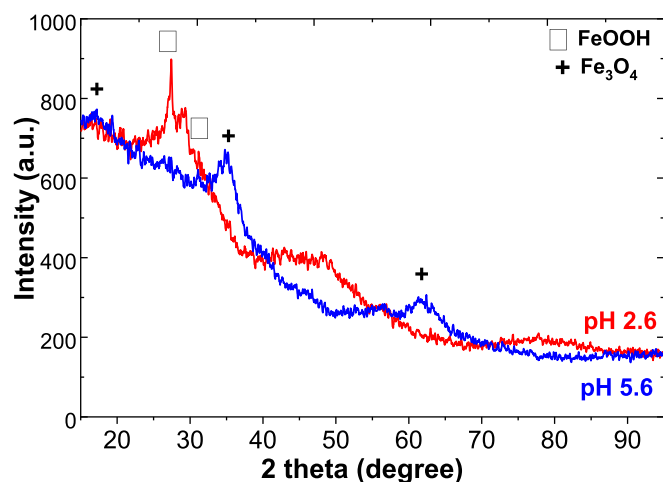

Fig. 5. Powder XRD spectra of the samples obtained by NH$_3$(aq) precipitation at various pH.

A series of experiments were conducted to determine the most suitable adsorbent for REEs extraction from supernatant. Table 8 shows the behaviour of adsorbents in the metal ions uptake from solutions pH near 4.5 during 1 h contact time. A stirring time was sufficient to attain ion adsorption equilibrium based on early report (Dudarko et al., 2021).

The total metal ions uptake of *SBA/EDTA/PO$_3$H$_2$* was approximately five times larger than that of other samples under the same pH (Table 8). These results are suggesting an outstanding adsorption property of *SBA/EDTA/PO$_3$H$_2$* for REEs. The adsorption capacity, of metal ions on *SBA/EDTA/PO$_3$H$_2$* follows the trend: Nd^{3+} > Fe^{3+} > Dy^{3+} > Ni^{2+}. In addition, *SiO$_2$/PO$_3$H$_2$* and *SBA/EDTA* samples showed the same order of preference. In contrast, the order of preference for metal ion adsorption by *SBA/EDTA/NH$_2$* sample is different Nd^{3+} ~ Ni^{2+} > Fe^{3+} ~ Dy^{3+}. The primary binding mechanisms of metal ions in the case of the *SBA/EDTA* sample are electrostatic interactions, ion-exchange reactions and chelating/coordination mechanism with ligands provided by EDTA groups. In an unprotonated state of the *SBA/EDTA/NH$_2$* sample the coordination of REEs ions occurs through N/O-donor ligand and by coordination mechanisms with aminopropyl groups which increase affinity toward Ni^{2+} ions in the multi-component solution.

Incorporation of P-containing groups into a silica network increases the affinity toward REEs in solution. This occurs via providing extra binding sites, selectivity and additional interactions with metal ions. Moreover, in spite of the fact that hydrogen bonds in complexonates such as EDTA groups are incomparably weaker than coordination bonds, the ring closure due to phosphonic groups probably makes an additional energetic contribution to the stabilization of structure. To some extent, this determines the structure of complexes on the silica surface of the *SBA/EDTA/PO$_3$H$_2$* sample. Differences in the adsorption behaviour of functionalized silica samples in the multi-component solution, compared to individual solutions, have been observed (Dudarko et al., 2021).

To confirm the interaction of metal ions with organic species on the adsorbents, FTIR spectra were performed (Fig. 8). The absorption bands of phosphonic groups (ν_{P-O} (1140–1240 cm^{-1})) overlap with the absorption bands of the silica skeleton (δ_{Si-OH} and $\delta_{Si-O-Si}$). Therefore, the IR spectra for *SBA/EDTA/PO$_3$H$_2$* and *SiO$_2$/PO$_3$H$_2$* samples are low informative on bonding type. The most representative bands of functionalized silica are present after 1200 cm^{-1} (**Fig. S5**) (Dudarko et al., 2021). The FTIR spectra of the as-synthesized and metal-adsorbed *SBA/EDTA/NH$_2$* samples are shown in Fig. 8. Since, the studied adsorbents contain hydrated protolithic active groups, to reduce the influence of water, the samples were thermally treated at FTIR measurements (25–140 °C). Only two bands of the silica matrix at 1861 and 1991 cm^{-1} appeared in this region. The band at 1720 cm^{-1} in *SBA/EDTA/NH$_2$* assigned to the stretching of the $\nu_{C=O}$ in the -COOH groups (non-ionized). The band at 1600 cm^{-1} (coordinated carboxyl groups), the long-wave wing of this band causes a shift of the δ_{HOH} band to 1648 cm^{-1}. This effect was confirmed after removal of water from silica matrix at 140 °C.

Metal ion removal from loaded silica-based adsorbents makes multiple changes in FTIR spectra in comparison with the spectra of the initial samples (Fig. 8). Namely, a several new adsorption peaks appear, which suggests adsorbents complexity. The absorption bands at 2850–3000 cm^{-1} in the spectra of all silica's before and after extraction of metal ions are assigned to characteristic ν_{C-H} bonds of the CH$_2$-groups. The wide peak at 1540 cm^{-1} is associated with deformation vibration of protonated N-containing ligands as results of zwitterion constitution of the functional groups (Han et al., 2007) on the surface of *SBA/EDTA/NH$_2$*. This band shifted to a lower frequency (1521 cm^{-1}) in the Metal-loaded adsorbent spectra indicating the coordination process by the N-containing groups in the solid phase of adsorbent. The participation of the carbonyl oxygen atom of the carboxylic group in coordination process between the ligand and the metal ions of simulated magnet solution appeared in the band shifted from 1648 cm^{-1} to 1630 cm^{-1} and from 1600 cm^{-1} to 1595 cm^{-1}, respectively. The bands in the 560–550 cm^{-1}
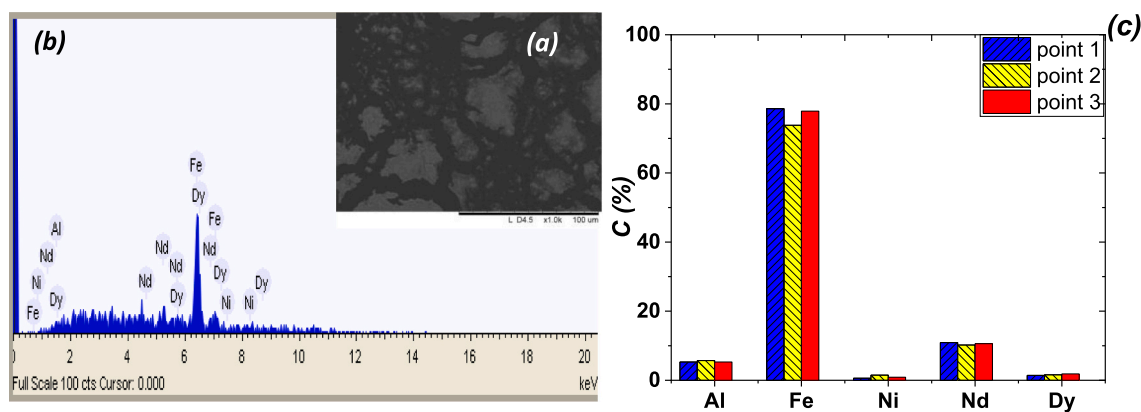
Fig. 6. SEM images (*a*), EDX spectrum (*b*) and analysis (*c*) of precipitate after treatment by $NH_{3(aq)}$ at pH = 2.5.

Table 7
Concentration of metal ions in supernatants before and after treatment by $NH_{3(aq)}$.

Operation	C, mmol L^{-1}					
	Nd^{3+}	Dy^{3+}	Fe^{3+}	Al^{3+}	B^{3+}	Ni^{2+}
Before treatment	27.7	2.76	59.4	0.27	5.71	4.01
1st treatment	22.02 ± 0.04	2.42 ± 0.06	11.61 ± 0.04	0.12 ± 0.06	5.42 ± 0.04	3.11 ± 0.07
2nd treatment	21.01 ± 0.02	2.22 ± 0.04	10.99 ± 0.03	0.19 ± 0.05	5.41 ± 0.03	3.01 ± 0.09
refluxing at 80 °C	22.01 ± 0.03	2.31 ± 0.05	10.62 ± 0.05	0.19 ± 0.04	5.42 ± 0.05	2.99 ± 0.05

Notes. pH = 2.5.

region are attributed to ν_{M-O} deformation (**Fig. S5**). The FTIR data therefore concluded the interaction of metal ions with functional groups of silica during complexation reaction, supporting the adsorption mechanism through the ionic exchange of Al^{3+} ions with surface NH^{3+}-groups.

According to **Table S2**, it was observed that Nd and Dy could be completely desorbed by 0.5 M HNO_3 treatment from the REEs-loaded adsorbents. For all experiments, REEs-loaded adsorbents were eluted by nitric acid. Chemical composition of eluting solution using various adsorbents was determined by ICP-OES (Table 9).

The amount of the REEs in the eluent is 97.0% and 89.7% for the $SBA/EDTA/PO_3H_2$ and SiO_2/PO_3H_2, respectively. Because highly selective separation of REEs from other impurities is difficult by the conventional static mode, separation of Nd and Dy is required in column (dynamic mode).

3.3.3. The reusability of adsorbents

Reusability of the adsorbents has been studied by evaluation of overall recovery REEs (Fig. 9), as it is important for the cost-effective use of materials in economically friendly hydrometallurgy process.

According to the comparison of data presented on Fig. 9, $SBA/EDTA/PO_3H_2$ sample can be used as adsorbent in repeated adsorption/desorption cycles using 0.5 M HNO_3 as desorption reagent. Rinsing of adsorbents between each sorption and desorption step was performed with double distilled water. Only insignificant degradation in adsorption efficiency was observed with $SBA/EDTA/PO_3H_2$. A significant decrease in the adsorbed amount on the SiO_2/PO_3H_2 sample, compared to $SBA/EDTA/PO_3H_2$ is due to the incomplete desorption of REEs from the sample. The reason for this behaviour is presumably the water-saturated and swellable non-ordered silica structure (xerogel). However, after complete desorption of REEs the adsorbents can be used again with the same effectiveness.

3.4. Procedure based on step-by-step SPE of interference and REEs

In the second stage, the hydrometallurgical process with step-by-step SPE was applied for REEs extraction from a simulated magnet solution. Thereupon, in initial stages of study various P/N-functionalized silica were utilized for REEs recovery from simulated solution with an aim to evaluate the effectiveness of adsorbents and select the most promising ones. A process flowsheet of REEs extraction based on step-by step SPE from simulated solution is presented in Fig. 10.

To investigate the adsorption behaviour of the studied adsorbents with respect to target REEs and other metal ions in simulated solution, we carried out adsorption experiments at an initial pH range from 2.0 to 2.5. Since, the P/N functionalized silica adsorbs negligible amounts of REEs in the acidic conditions (Dudarko et al., 2021), whereas Fe^{3+} ions extract at pH_{eq} value near 2.0. Adsorption performances of the studied adsorbents with regard to metal ions are summarized in Table 10.

From the data presented in Table 10, it is clear that bare silica (*SBA* sample) demonstrated null uptake for REEs, while Fe^{3+} ions were adsorbed with poor efficiency. In a global sense, the silica displayed good uptake toward Fe^{3+} (not for Dy^{3+} or Nd^{3+}) in the current system, irrespective of the type of adsorbents. Really, the affinity of the adsorbents toward Fe^{3+} ions in acidic medium was higher than that toward REEs ions (Table 5).

In general, the descending order of efficiencies of adsorbents studied in this work is $SBA/EDTA/PO_3H_2 > SiO_2/PO_3H_2 >> SBA/EDTA \approx SBA/EDTA/NH_2 >> SBA$. Taking into account the characteristics of $SBA/EDTA/PO_3H_2$ and $SBA/EDTA$ samples examined herein, we considered that higher selectivity to Fe^{3+} ions could be attributed to the chelation mechanism with EDTA groups of silica matrix. The $SBA/EDTA/PO_3H_2$ sample manifest better characteristics than the SiO_2/PO_3H_2, being more efficient and selective adsorbents for Fe^{3+} at pH 2.0 in multi-component solution allowing the separation of REEs. The interfering Ni^{2+} and Al^{3+} ions did not adsorb on SiO_2/PO_3H_2 sample under low pH (**Fig. S6**). These results are interesting and very important for the extraction of target REEs from multi-component solution such as the simulated magnet solution. At low pH, the mesoporous networks of $SBA/EDTA/NH_2$ adsorbent likely had a higher amount of cationic forms because most of the NH_2-groups were converted into $-NH_3^+$ groups. Thus, Fe^{3+} (or REEs) ions would be repelled from the adsorbent's positively charged surface, resulting in low capacity for Fe^{3+} (or REEs) uptake. Thus, for $SBA/EDTA/NH_2$ adsorbent it was realized that only EDTA groups contributed to the adsorption of Fe^{3+}. The $SBA/EDTA/NH_2$ sample showed a greater level of Fe^{3+} ions removal compared to the bare silica matrix. So, most abundant macro impurity in the magnet solution (Fe^{3+} ions) should be removal before recovery of target REEs by SPE method (Table 11).

3.4.1. Recovery of REEs

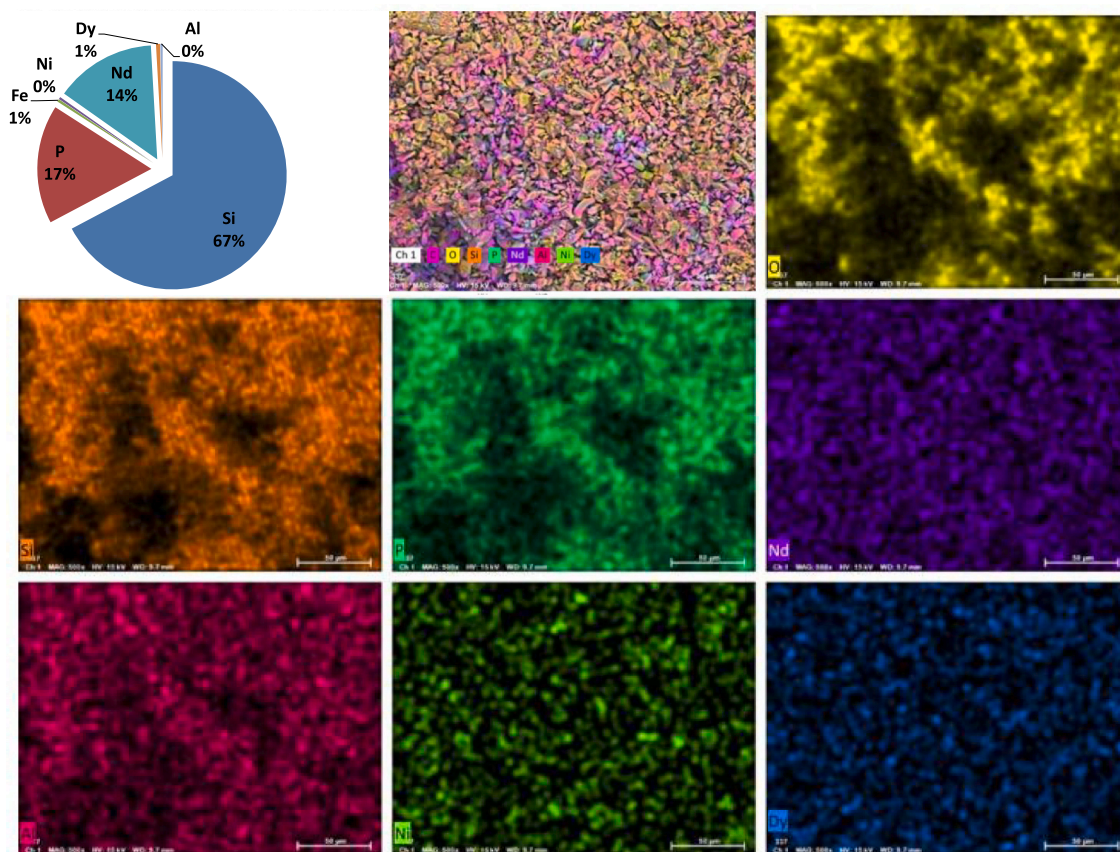The extraction of REEs from multi-component mixture by SPE was

Fig. 7. EDX mappings distribution and its associated elemental analysys of SiO_2/PO_3H_2 sample after adsorption from supernatant after treatment by NH_3(aq).

Table 8
Performance of adsorbents toward metal ions in supernatant after precipitation.

Sorbent	pH$_0$	q$_e$, mg g^{-1} (mmol g^{-1})			
		Fe^{3+}	Ni^{2+}	Dy^{3+}	Nd^{3+}
SBA/EDTA	5.61	5.04 (0.09)	8.01 (0.13)	3.25 (0.02)	11.5 (0.08)
SBA/EDTA/ PO$_3$H$_2$	5.50	56.4 (1.11)	1.17 (0.02)	3.52 (0.06)	171 (1.19)
SBA/EDTA/NH$_2$	5.65	12.3 (0.01)	6.45 (0.11)	1.17 (0.02)	14.4 (0.10)
SIO$_2$/PO$_3$H$_2$	5.39	27.4 (0.49)	0.59 (0.02)	2.93 (0.05)	39.8 (0.58)

Notes. n.d. –not detected.

conducted when qualitative reaction for Fe^{3+} ions ($Fe^{3+} + 3SCN^- \rightarrow Fe(SCN)_3$) was negative. Thus, we investigated SPE of REEs from the simulated solution after removal of Fe^{3+} ions. The optimum pH value for the removal of REEs by silica based adsorbents from aqueous solution ranged from 3.5 to 6.0 (Dudarko et al., 2021). In this pH range, neither precipitation of the metal hydroxide (Fig. 2) nor protonation of the N-containing groups of adsorbents is expected. In order to achieve high efficiency pH 5.5 (natural pH) was selected for subsequent work. In this case, the supernatant solution obtained after removal of Fe (as main impurity) from the simulated magnet solution was used as the feed solution for REEs removal with pH ~ 5.5, which was adjusted by alkali aqueous solution. After that, the adsorbent was centrifuged and the liquid was sampled for ICP-OES analysis (Table 12). The solids were also washed and analysed.-

In order to achieve complete extraction of REEs, it was necessary to extract ions from the simulated solution two times. After the first run the effluent contained trace amount of Ni^{2+} ions. Hence, two cycles were
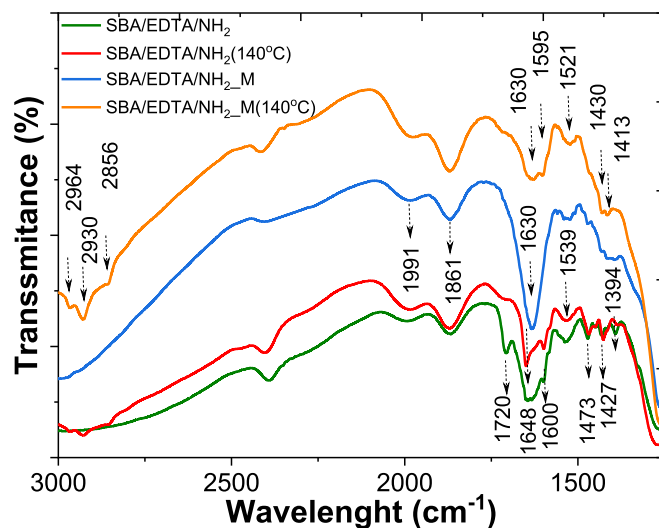

Fig. 8. Fragment of FTIR spectra of initial $SBA/EDTA/NH_2$ and metal-loaded ($SBA/EDTA/NH_2$_M) samples.

Table 9
Distribution of metal ions in eluting solution of $SBA/EDTA/PO_3H_2$ and SiO_2/PO_3H_2 samples.

Adsorbent	ϖ, %					
	Fe^{3+}	Al^{3+}	Nd^{3+}	Ni^{2+}	Dy^{3+}	B^{3+}
SBA/EDTA/PO$_3$H$_2$	1.1	0.7	88.9	0.1	8.1	1.1
SiO$_2$/PO$_3$H$_2$	3.1	3.2	81.5	2.0	8.2	2.0
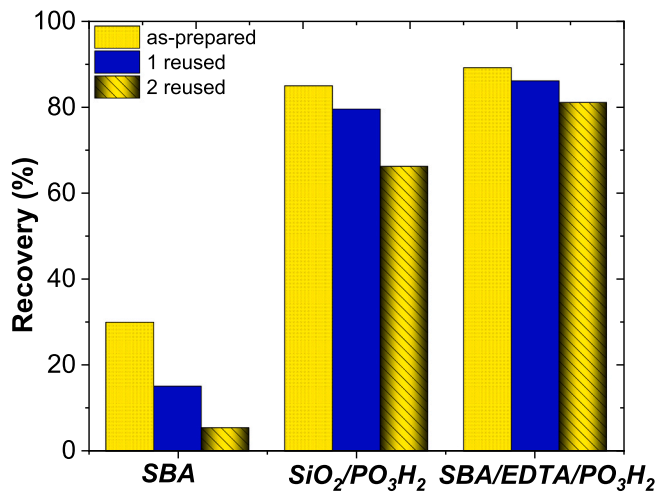
Fig. 9. Regeneration cycles of studied adsorbents for REEs.

Table 10
Adsorption performance of adsorbents in initial simulated magnet solution.

Sample	pH_{eq}	q_e, mg g^{-1} (mmol g^{-1})			
		Fe^{3+}	Ni^{2+}	Dy^{3+}	Nd^{3+}
SBA	2.15	0.56 (0.01)	n.d.	n.d.	1.44 (0.01)
SBA/EDTA	2.05	13.44 (0.24)	1.76 (0.03)	3.25 (0.02)	7.25 (0.05)
SBA/EDTA/ PO₃H₂	2.15	62.19 (1.11)	1.17 (0.02)	9.75 (0.06)	17.28 (0.12)
SBA/EDTA/NH₂	2.07	1.68 (0.03)	5.87 (0.10)	3.25 (0.02)	1.44 (0.01)
SiO₂/PO₃H₂	2.11	27.44 (0.49)	1.17 (0.02)	8.13 (0.05)	46.08 (0.32)

Notes. n.d. –not detected.

selected for further experiments. The results are shown in Table 13.

As shown in Table 13, the extraction efficiency of REEs by both adsorbents was more than 93%. The degree of Fe^{3+} ions extraction degree into the solid phase of bifunctional adsorbent is significantly less compared to the monofunctional solid (SiO_2/PO_3H_2) and does not exceed 0.7%. The Ni^{2+} ions were not observed in eluate of SiO_2/PO_3H_2 because this adsorbent is unselective toward transition element (Table 5). The eluent of both adsorbents contain B^{3+}. It is probably related to that major part of B^{3+} in anionic form as counterion of target metal ions in solutions.

The concentrations of Nd, and Dy in the outlet were significantly enhanced with the gradient elution in dynamic conditions. The ability to

extraction REEs by this process is seen possible, since, adsorption of REEs (Dy, Nd) is suppressed by decreasing the pH value of the solution, while adsorption of Fe increased on the surface of $SBA/EDTA/PO_3H_2$. The gradient elution using HNO_3 solution was performed with the Me-loaded adsorbents in column. In the case of pH 3.0, the elution amount Nd is maximum, and the purity of Nd in the eluent is 98.4%.

Procedure based on step-by-step SPE treatments induce higher extraction and selectivity toward REEs than the approach which used precipitation for the removal of impurities.

3.5. Recovery of REEs from leaching solution of real NdFeB magnets

It is vitally important to apply the developed procedures and possibility for direct recovery of REEs from the real NdFeB magnet. The NdFeB magnets from Jin Tong Magnet (China) with the diameter of 75 mm and thickness of 5 mm were used in these experiments. Chemical composition of the initial permanent magnet sample is given in
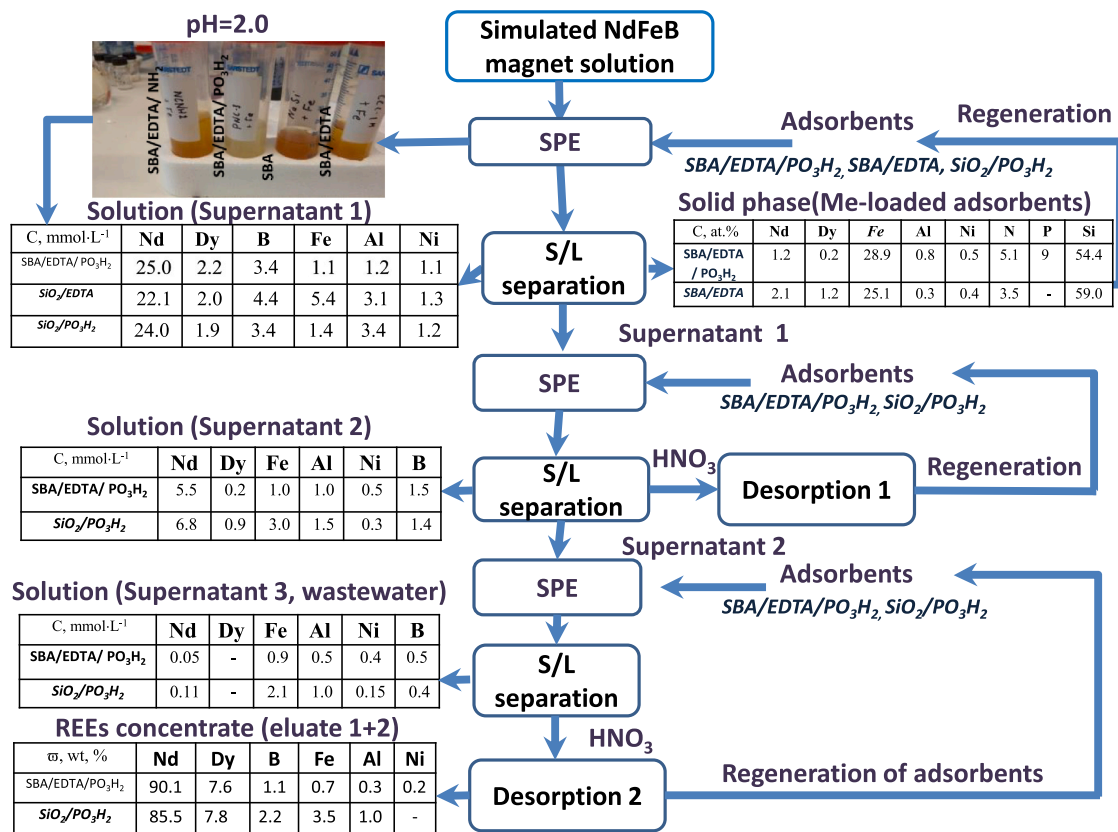

Fig. 10. Hydrometallurgical process for REEs recovery based on step-by-step SPE from simulated solution.

Table 11
Composition of supernatant after SPE with different adsorbents.

Sorbent	Treatment	C, mmol L^{-1}					
		Nd^{3+}	Dy^{3+}	Fe^{3+}	Al^{3+}	Ni^{2+}	B^{3+}
SBA/ EDTA/ PO_3H_2	1st	22.02 ± 0.04	2.42 ± 0.06	1.10 ± 0.02	0.10 ± 0.06	1.22 ± 0.04	2.81 ± 0.05
	2 nd	25.04 ± 0.02	2.24 ± 0.04	1.07 ± 0.03	0.22 ± 0.05	1.25 ± 0.05	2.43 ± 0.06
SiO_2/ PO_3H_2	1st	24.21 ± 0.04	2.02 ± 0.06	1.51 ± 0.03	3.52 ± 0.07	1.26 ± 0.06	4.11 ± 0.08
	2 nd	22.11 ± 0.02	1.91 ± 0.04	1.43 ± 0.04	3.41 ± 0.06	1.21 ± 0.04	3.41 ± 0.07
SBA/ EDTA	1st	22.13 ± 0.06	2.06 ± 0.08	1.74 ± 0.05	3.13 ± 0.04	1.23 ± 0.07	4.44 ± 0.08

Notes. Based on ICP-OES data (pH 2.0).

Table 12
Comparison of adsorption capacity toward REEs by several adsorbents from studied mixture.

Sorbent	Treatment	pH_o	Nd^{3+}			Dy^{3+}		
			q_e, mg g^{-1}	q_e, mmol g^{-1}	Recovery, %	q_e, mg g^{-1}	q_e, mmol g^{-1}	Recovery, %
$SBA/EDTA/PO_3H_2$	1st	5.48	170.6	1.2	85.6	7.6	0.05	67.4
	2 nd	5.48	32.3	0.2	99.6	6.5	0.04	99.6
SiO_2/PO_3H_2	1st	5.36	149.0	1.0	74.7	6.3	0.04	56.5
	2 nd	5.36	45.2	0.3	99.6	8.7	0.05	99.6

Table 13
Distribution of metal ions in eluting solution of $SBA/EDTA/PO_3H_2$ and SiO_2/PO_3H_2 samples.

Adsorbent	ϖ, %					
	Fe^{3+}	Al^{3+}	Nd^{3+}	Ni^{2+}	Dy^{3+}	B^{3+}
$SBA/EDTA/PO_3H_2$	0.7	0.3	90.1	0.2	7.6	1.1
SiO_2/PO_3H_2	3.5	1.0	85.5	–	7.8	2.2

Table 14.

In this case, developed procedure based on step-by-step SPE was used for the recovery of REEs. The sample of NdFeB magnet after leaching was analysed according to the flow-sheet shown in *Schema 3*.

The dissolution of NdFeB magnets were investigated with chemical leaching. In a selective leaching process, the first step is commonly the complete leaching of magnets by 0.5 M H_2SO_4. For leaching experiments three-necked glass flask (100 mL) enclosed with access for mechanical stirring was used for tests. The leaching efficiency increased 3 times after applying ultrasonic treatment during 5 to 30 min without heating, which allowed complete dissolution of NdFeB magnet. Various ratios of magnet-to-acid were also studied (Table 15).

Neutralization of acidic solution by NaOH (1 M) was utilized for pH regulation. After adjustment of pH, the adsorbents ($SBA/EDTA/PO_3H_2$ or $SBA/EDTA$) were immersed in the pregnant leach liquor, and then separated by centrifugation. Then, the adsorbents ($SBA/EDTA/PO_3H_2$ or SiO_2/PO_3H_2) were immersed in the supernatant solution and separated after SPE. The loaded adsorbents were rinsed and, finally, the eluting solution was added. The concentration of metal ions was determined in the pregnant leach solution and eluted solutions, as well as in supernatant after adsorption. According to the multi-element analysis the leach liquor mainly consists of REEs (Nd, Dy and Pr) and impurities (Fe, Ni, Al and B), Table 15. Application of $SBA/EDTA/PO_3H_2$ and $SBA/$

$EDTA$ samples at pH = 2.0 allowed the recovery 63% of REEs from acidic leach liquor of magnet. After two contcats of $SBA/EDTA/PO_3H_2$ and SiO_2/PO_3H_2 adsorbent samples with the leach liquor at pH = 5.5 and elution with HNO_3 in the column allowed the recovery 97.1% and 94.9% of REEs, respectively, determined in the supernatant of leaching solution of NdFeB magnet (Fig. 11).

These results are consistent with the results based on simulated solutions shown in Tables 12. It is important to mention that regardless of the essential difference in volume of leaching solutions, the amount of the extracted REEs is almost the same (*Fig. S7*). Thus, it confirms the appropriateness of the developed step-by-step SPE procedure and precision of the full permanent magnet analysis. The total price of adsorbents indicated the use of SiO_2/PO_3H_2 sample considerably decrease the cost of synthesis by 50% (*Table S1*) with high recovery of REEs (Fig. 11). Also, these results demonstrate the potential of use of functionalized silica-based materials for recycling of EOL permanent magnets.

4. Conclusions

In summary, several mono- and bi-functional mesoporous silica functionalized by phosphonate and aminopolycarboxylate groups were shown to be highly effective adsorbents for the selective removal of REEs from simulated magnet solution and leach solution produced from them NdFeB magnet. Meanwhile, the major impurity (e.g. Fe) of simulated magnet solution and other minor impurities (e.g. Al, Ni, B) were eliminated through precipitation by pH adustments using ammonia solution or SPE at pH near 2.0. The extraction of REEs from supernatant was performed from neutral media containing trace amount Al^{3+}, Ni^{2+} and borate as impurities using SPE by silica adsorbents. The mechanisms of metal ions (REEs and impurities) interaction during their extraction by functional groups of silica adsorbents were identified and discussed. The efficiency extraction of REEs using the mesoporous silica functionalized by EDTA and/or phosphonic groups (P,N,O-complexonates) is much higher than that modified with EDTA in combination with NH_2-groups under the same conditions. The proposed procedure based on step-by-step SPE treatments using mesoporous silica functionalized by P,N,O-complexonates induce to higher recovery (97.1%) of REEs from pregnant leach liquor of the industrial NdFeB magnet. The separation of Nd^{3+} and Dy^{3+} was performed in nitric acid media using the gradient elution in column. Regeneration of adsorbents was achieved with HNO_3, without reduction of adsorption performance in the several reuse cycles. We have demonstrated that the studied functionalized mesoporous materials have great potential for technological application in recycling EOL materials (magnet, LEDs, HDD, fluorescent lamps, electric motors and generators for wind turbines). For the efficient recycling of REEs from magnet waste proposed hydrometallurgical process is convenient and green, which possess a good reproducibility.

CRediT authorship contribution statement

Oksana Dudarko: Formal analysis, Investigation, Data curation, Writing – original draft. **Natalia Kobylinska:** Conceptualization, Methodology, Investigation, Data curation, Resources, Writing – review

Table 14
Chemical composition of the starting real permanent magnet.

Element	Al	B	Ni	Dy	Fe	Nd	Pr	Other	Total
wt%	1.01	1.02	0.42	3.93	63.9	22.3	5.98	1.44	100

Table 15
Composition of the pregnant leach solution after dissolution of NdFeB magnet in bulk form.

Sample	C, mmol L^{-1}						
	Nd^{3+}	Dy^{3+}	Pr^{3+}	Fe^{3+}	Ni^{2+}	Al^{3+}	B^{3+}
NdFeB/100	15.5	2.42	4.24	114.1	0.72	3.74	9.44
NdFeB/200*	7.73	1.22	2.10	57.1	0.35	1.87	4.72

Notes. Leaching conditions: 100 mL or 200 mL of 0.5 M H$_2$SO$_4$ for 30 min at room temperature using ultrasonic treatment over 30 min.
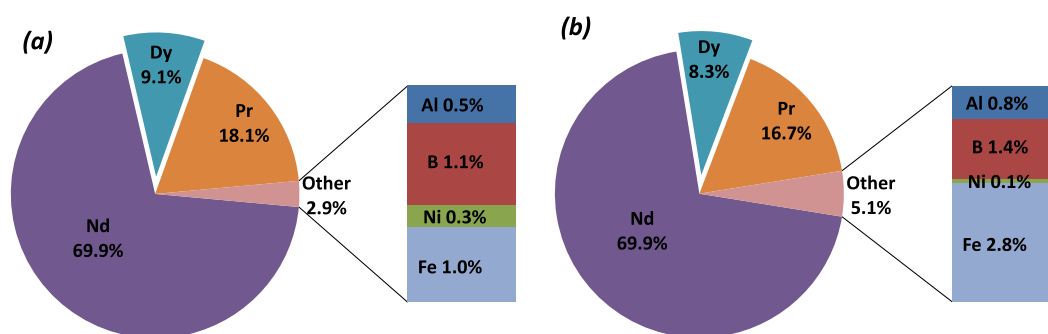
Fig. 11. Distribution of metal ions in eluting solution of *SBA/EDTA/PO$_3$H$_2$* (a) and *SiO$_2$/PO$_3$H$_2$* (b) samples after SPE from leach liquor of real magnet.

Appendix B. Supplementary data

Supplementary material related to this article (**Fig. S1-S7, Table S1-S2**) can be found in the online version. Supplementary data to this article can be found online at https://doi.org/10.1016/j.hydromet.2022.10 5855.

References

Alonso, E., Sherman, A.M., Wallington, T.J., Everson, M.P., Field, F.R., Roth, R., Kirchain, R.E., 2012. Evaluation rare earth element availability: a case with revolutionary demand from clean technologies. Environ. Sci. Technol. 46, 3406–3414. https://doi.org/10.1021/es203518d.
Anastopoulos, I., Bhatnagar, A., Lima, E.C., 2016. Adsorption of rare earth metals: a review of recent literature. J. Mol. Liq. 221, 954–962.
Anderegg, G., 1977. Critical Survey of Stability Constants of EDTA Complexes: Critical Evaluation of Equilibrium Constants in Solution: Stability Constants of Metal Complexes. Pergamon Press. https://doi.org/10.1016/C2013-0-02924-6
Auerbach, R., Bokelmann, K., Stauber, R., Gutfleisch, O., Schnell, S., Ratering, S., 2019. Recycling of rare earth metals out of end of life magnets by bioleaching with various bacteria as an example of an intelligent recycling strategy. Miner. Eng. 134, 104–117.
Baerlocher, Ch., McCusker, L.B., Olson, D.H., 2007. Atlas of Zeolite Framework Types, Sixth Edition: 6. Elsevier Science, 404 p.
Banda, R., Jeon, H., Lee, M., 2012. Solvent extraction separation of Pr and Nd from chloride solution containing La using Cyanex 272 and its mixture with other extractants. Sep. Purif. Technol. 98, 481–487. https://doi.org/10.1016/j.seppur.2012.08.015.
Barrett, E.P., Joyner, L.G., Halenda, P.P., 1951. The determination of pore volume and area distributions in porous substances. I. Computations from nitrogen isotherms. J. Am. Chem. Soc. 373–380.
Binnemans, K., Tom Jones, P., Blanpain, B., Van Gerven, T., Yang, Y., Walton, A., Buchert, M., 2013. Recycling of rare earths: a critical review. J. Clean. Prod. 51, 1–22.
Brunauer, J.S., Emmet, P.H., Teller, E., 1938. Adsorption of gases in multimolecular layers. J. Am. Chem. Soc. 60, 309–319. https://doi.org/10.1021/ja01269a023.
Dabrowski, A., Barczak, M., Dudarko, O.A., Zub, Yu.L., 2007. Preparation and characterization of polysiloxane xerogels having covalently attached phosphoric groups. Pol. J. Chem. 81 (4), 475–483.
Descriptive Inorganic Chemistry Researches of Metal Compounds (Ed.), 2017. Edited by T. Akitsu. Intech Open. https://doi.org/10.5772/65855.
du Preez, A.C., Preston, J.S., 1992. The solvent extraction of rare-earth metals by carboxylic acids. Solvent Extr. Ion Exch. 10, 207–230. https://doi.org/10.1080/07366299208918101.
Dudarko, O., Zub, Y., 2017. Synthesis of SBA-15 type organosilica sorbents using sodium metasilicate and phosphonic acid residues. Chem. J. Moldova. General, Industrial and Ecological Chemistry. 12 (2), 79–86. https://doi.org/10.19261/cjm.2017.417.

Dudarko, O., Kobylinska, N., Mishra, B., Kessler, V.G., Tripathi, B.P., Seisenbaeva, G.A., 2021. Facile strategies for synthesis of functionalized mesoporous silicas for the removal of rare-earth elements and heavy metals from aqueous systems. Microporous Mesoporous Mater. 315, 110919 https://doi.org/10.1016/j.micromeso.2021.110919.

Firdaus, M., Rhamdhani, M.A., Durandet, Y., Rankin, W.J., McGregor, K., 2016. Review of high-temperature recovery of rare earth (Nd/Dy) from magnet waste. J Sustain Metall. 2, 276–295. https://doi.org/10.1007/s40831-016-0045-9.

Galarneau, A., Cambon, H., Di Renzo, F., Fajula, F., 2001. True microporosity and surface area of mesoporous SBA-15 Silicas as a function of synthesis temperature. Langmuir 17, 8328–8335. https://doi.org/10.1021/la0105477.

Gergoric, M., Ekberg, C., Steenari, B.M., Vollmer, T.R., 2017a. Separation of heavy rare-earth elements from light rare-earth elements via solvent extraction from a neodymium magnet leachate and the effects of diluents. J. Sustain. Metall. 3, 601–610. https://doi.org/10.1007/s40831-017-0117-5.

Gergoric, M., Ekberg, Ch., Foreman, M.R.St.J., Steenari, B.-M., Retegan, T., 2017b. Characterization and leaching of neodymium magnet waste and solvent extraction of the rare-earth elements using TODGA. J. Sustain. Metall. 3, 638–645. https://doi.org/10.1007/s40831-017-0122-8.

Han, L., Ruan, J., Li, Y., Terasaki, O., Che, Sh., 2007. Synthesis and characterization of the amphoteric amino acid bifunctional mesoporous silica. Chem. Mater. 19 (11), 2860–2867. https://doi.org/10.1021/cm0705845.

Herbst, J.F., Croat, J.J., 1991. Neodymium-iron-boron permanent magnets. J. Magn. Magn. Mater. 100, 57–78.

Hoogerstraete, T.V., Blanpain, B., Van Gerven, K., Binnemans, T., 2014. From NdFeB magnets towards the rare-earth oxides: a recycling process consuming only oxalic acid. RSC Adv. 4, 64099–64111. https://doi.org/10.1039/C4RA13787F.

Hu, Y., Florek, J., Lariviere, D., Fontaine, F.-G., Kleitz, F., 2018. Recent advances in the separation of rare earth elements using mesoporous hybrid materials. Chem. Rec. 18, 1261–1276. https://doi.org/10.1002/tcr.201800012.

Humphries, M., 2013. Rare earth elements: The global supply chain. In: Congressional Research Service, 7–5700, R41347. USA, Washington. www.crs.gov.

Judge, W.D., Azimi, G., 2020. Recent progress in impurity removal during rare earth element processing: a review. Hydrometallurgy 196, 105435. https://doi.org/10.1016/j.hydromet.2020.105435.

Jyothi, R.K., Thenepalli, T., Ahn, J.W., Parhi, P.K., Chung, K.W., Lee, J.-Y., 2020. Review of rare earth elements recovery from secondary resources for clean energy technologies: grand opportunities to create wealth from waste by saving energy. J. Clean. Prod. 267, 122048.

Khoe, G.H., Brown, P.L., Sylva, R.N., 1986. The hydrolysis of metal ions. Part 9. Iron (III) in perchloric, nitrate, and chloride media (1 Mol dm^{-3}). J. Chem. Soc. Dalton Trans. 9, 1901–1906.

Kikuchi, Y., Matsumiya, M., Kawakami, S., 2014. Extraction of rare earth ions from Nd-Fe-B magnet wastes with TBP in Tricaprylmethylammonium nitrate. Solvent Extraction Research and Development, Japan. 21 (2), 137–145. https://doi.org/10.15261/serdj.21.137.

Kim, D., Powell, L.E., Delmau, L.H., Peterson, E.S., Herchenroeder, J., Bhave, R.R., 2015. Selective extraction of rare earth elements from permanent magnet scraps with membrane solvent extraction. Environ. Sci. Technol. 49 (16), 9452–9459. https://doi.org/10.1021/acs.est.5b01306.

Krupińska, I., 2019. Removal of iron and organic substances from groundwater in an alkaline medium. J. Environ. Eng. Landsc. Manag. 27 (1), 12–21. https://doi.org/10.3846/jeelm.2019.7726.

Makarova, I., Soboleva, E., Osipenko, M., Kurilo, I., Laatikainen, M., Repo, E., 2020. Electrochemical leaching of rare-earth elements from spent NdFeB magnets. Hydrometallurgy 192, 105264.

Nordstrom, D.K., 2000. Advances in the hydrogeochemistry and microbiology of acid mine waters. Int. Geol. Rev. 42, 499–515. https://doi.org/10.1080/00206810009465095.

Ogata, T., Narita, H., Tanaka, M., 2015. Adsorption behavior of rare earth elements on silica gel modified with diglycol amic acid. Hydrometallurgy 152, 178–182.

Ogata, T., Narita, H., Tanaka, M., 2016. Adsorption mechanism of rare earth elements by adsorbents with diglycolamic acid ligands. Hydrometallurgy 163, 156–160.

Okabe, T.H., Takeda, O., Fukuda, K., Umetsu, Y., 2003. Direct extraction and recovery of neodymium metals from magnet scrap. Mater. Trans. 44, 798–801.

Önal, M.A.R., Borra, C.R., Guo, M., Blanpain, B., Gerven, T.V., 2015. Recycling of NdFeB magnets using sulfation, selective roasting, and water leaching. J. Sustain. Metall. 1, 199–215.

Pradhan, S., Swain, N., Prusty, S., Kumar Sahu, R., Mishra, S., 2020. Role of extractants and diluents in recovery of rare earths from waste materials. Mater. Today: Proceedings. 20 (part 2), 239–245. https://doi.org/10.1016/j.matpr.2020.01.288.

Queffélec, C., Petit, M., Janvier, P., Knight, D.A., Bujoli, B., 2012. Surface modification using Phosphonic acids and esters. Chem. Rev. 112, 3777–3807. https://doi.org/10.1021/cr2004212.

Rabatho, J.P., Tongamp, W., Takasaki, Y., Haga, K., Shibayama, A., 2013. Recovery of Nd and Dy from rare earth magnetic waste sludge by hydrometallurgical process. J. Mater. Cycles Waste Manag. 15, 171–178.

Riano, S., Binnemans, K., 2015. Extraction and separation of neodymium and dysprosium from used NdFeB magnets: an application of ionic liquids in solvent extraction towards the recycling of magnets. Green Chem. 17, 2931–2942. https://doi.org/10.1039/C5GC00230C.

Roosen, J., Binnemans, K., 2014. Adsorption and chromatographic separation of rare earths with EDTA- and DTPA-functionalized chitosan biopolymers. J. Mater. Chem. A 2, 1530–1540.

SIST EN 60404–8-1, 2015. Magnetic materials - Part 8–1: Specifications for individual materials - Magnetically hard materials.

Stefaänsson, A., 2007. Iron(III) hydrolysis and solubility at 25 °C. Environ. Sci. Technol. 41, 6117–6123.

Tunsu, C., Petranikova, M., Gergoric, M., Ekberg, C., Retegan, T., 2015. Reclaiming rare earth elements from end-of-life products: a review of the perspectives for urban mining using hydrometallurgical unit operations. Hydrometallurgy 156, 239–258.

van Loy, S., Önal, M.A.R., Binnemans, K., van Gerven, T., 2020. Recovery of valuable metals from NdFeB magnets by mechanochemically assisted ferric sulfate leaching. Hydrometallurgy 191, 105154–105163. https://doi.org/10.1016/j.hydromet.2019.105154.

Venkatesan, P., Hoogerstraete, T.V., Hennebel, T., Binnemans, K., Sietsma, J., Yang, Y., 2018. Selective electrochemical extraction of REEs from NdFeB magnet waste at room temperature. Green Chem. 20, 1065–1073.

Wang, J., Liu, X., Fu, J., Xie, M., Huang, G., Wang, H., 2019. Novel extractant (2,4-dimethylheptyl)(2,4,4'-trimethylpentyl)phosphinic acid (USTB-2) for rare earths extraction and separation from chloride media. Sep. Purif. Technol. 209, 789–799.

Wellens, S., Thijs, B., Binnemans, K., 2012. An environmentally friendlier approach to hydrometallurgy: highly selective separation of cobalt from nickel by solvent extraction with undiluted phosphonium ionic liquids. Green Chem. 14, 1657–1665.

Yamada, E., Murakami, H., Nishihama, S., Yoshizuka, K., 2018. Separation process of dysprosium and neodymium from waste neodymium magnet. Sep. Purif. Technol. 192, 62–68. https://doi.org/10.1016/j.seppur.2017.09.062.

Yang, Y., Walton, A., Sheridan, R., Güth, K., Gauß, R., Gutfleisch, O., Buchert, M., Steenari, B.-M., Van Gerven, T., Jones, P.T., Binnemans, K., 2017. REE recovery from end-of-life NdFeB permanent magnet scrap: a critical review. J. Sustain. Metall. 3, 122–149. https://doi.org/10.1007/s40831-016-0090-4.

Yao, Y., Farac, N.F., Azimi, G., 2017. Supercritical fluid extraction of rare earth elements from nickel metal hydride battery. ACS Sustain. Chem. Eng. 6, 1417–1426. https://doi.org/10.1021/acssuschemeng.7b03803.

Yoon, H.-S., Kim, C.-J., Chung, K.-W., Kim, S.-D., Lee, J.-Y., Kumar, J.R., 2016. Solvent extraction, separation and recovery of the dysprosium (Dy) and neodymium (Nd) from aqueous solutions: waste recycling strategies for permanent magnet processing. Hydrometallurgy 165, 27–43.

Zakotnik, M., Harris, I.R., Williams, A.J., 2007. Possible methods of recycling NdFeB-type sintered magnets using the HD/degassing process. J. Alloys Compd. 450, 525–553. https://doi.org/10.1016/j.jallcom.2007.01.134.

Zawisza, B., Pytlakowska, K., Feist, B., Polowniak, M., Kita, A., Sitko, R., 2011. Determination of rare earth elements by spectroscopic techniques: a review. J. Anal. At. Spectrom. 12 (26), 2373–2390. https://doi.org/10.1039/C1JA10140D.

Zhang, J., Anawati, J., Yao, Y., Azimi, G., 2018. Aeriometallurgical extraction of rare earth elements from a NdFeB magnet utilizing supercritical fluids. ACS Sustain. Chem. Eng. 6, 16713–16725.

Zhang, W., Yu, Sh., Zhang, Sh., Zhou, J., Ning, Sh., Wang, X., Wei, Yu., 2019. Separation of scandium from the other rare earth elements with a novel macro-porous silica-polymer based adsorbent HDEHP/SiO$_2$-P. Hydrometallurgy 185, 117–124. https://doi.org/10.1016/j.hydromet.2019.01.012.

Zhu, Z.X., Sasaki, Y., Suzuki, H., Suzuki, S., Kimura, T., 2004. Cumulative study on solvent extraction of elements by N,N,N',N'-tetraoctyl-3-oxapentanediamide (TODGA) from nitric acid into n-dodecane. Anal. Chim. Acta 527, 163–168. https://doi.org/10.1016/j.aca.2004.09.023.